stants to the spin Hamiltonian exhibit the inequalities $g_{\parallel}>g_{\perp}$ and $D<0$, while calculations based on the crystalline electric field potential given by Eq. (1), the α-Al_2O_3 structure parameters and the assumption that $\lambda=-285$ cm^{-1}, reverse these inequalities and yield values of $(g-2)$ which are in the neighborhood of 300% greater than those determined experimentally. In a similar manner, a calculation of $(1/D)\partial D/\partial t$ based upon the room temperature thermal expansion coefficient for α-Al_2O_3 yields a value which is 200 to 300% smaller than the value observed at this temperature.

It thus appears that if a satisfactory explanation to these two behaviors and the appearance of the satellite resonance absorption is forthcoming, the simple model must of necessity be modified to take account of distortions produced by the large divalent nickel ion, the localization of charge compensators and the interaction with ions outside the oxygen octahedron.

ACKNOWLEDGMENTS

In conclusion, the authors would like to express their indebtedness to Mr. E. A. Fagen for his efforts in the design and construction of low temperature apparatus and spectrometer, to Mr. D. Mergerian for valuable experimental assistance, and to Mr. V. Rehn for helpful suggestions.

PHYSICAL REVIEW VOLUME 125, NUMBER 2 JANUARY 15, 1962

Knight Shift in Silver Base Solid Solutions

T. J. ROWLAND*
Technology Department, Union Carbide Metals Company, Niagara Falls, New York
(Received August 17, 1961)

This paper describes an experimental investigation of some primary substitutional solid solutions of silver. Nuclear magnetic resonance was used to detect the charge density at the solvent nuclei in these alloys, and the results are compared with theory. Solutes chosen for the study were Cu, Zn, Ga, Ge, As, Cd, In, Sn, Sb, Au, and Tl. Insertion of a few percent of any of these caused a decrease in the Knight shift of silver in rough proportion to both solute concentration and valence. Also the normally narrow silver absorption became very broad under the influence of a few percent solute. This severe broadening serves as the major basis for an argument concerning the distribution of charge density around the solute atoms. It is shown that dipolar and indirect exchange broadening are not sufficient to account for the observed linewidths; subsequently the absorption is analyzed in terms of the long-range oscillations in the conduction electron density thought to be present in the vicinity of the solute atoms. The comparison with theory indicates that the line shift and width are equally well explained by the presence of long-range oscillations. If the shift were much greater than that observed it would suggest another source of shift not included by the present mechanism. It is concluded that the theory of Blandin, Daniel, and Friedel is applicable to these alloys and explains the data satisfactorily. It is not possible to test the theory quantitatively unless one knows the exact phase shifts to describe the scattering process underlying this theory.

I. INTRODUCTION

THE purpose of this paper is to describe the results of an investigation of the nuclear magnetic resonance of Ag^{109} in an extensive group of silver base solid solutions. Early work directed at determining the dependence of the Knight shift on the constitution of solid solutions failed in that objective because of the dominant effect of quadrupole perturbations on the resonance in the systems considered. When it was recognized that localized conduction electron charge redistribution was responsible for these quadrupole interactions[1] the prospect of studying localized charge distributions by means of the Knight shift became attractive. It was also necessary to establish with certainty the dominant features to be associated with the effect of the Knight shift in alloys in order to consider their role in the analysis of the quadrupole interaction studies.[1] For the work reported here Ag^{109} was chosen for attention primarily because it has no nuclear electric quadrupole moment. Of course it was also advantageous that numerous solutions could be formed using silver as solvent. The electron distribution suggested and developed by Friedel and co-workers[2–4] will be used to analyze the data after it has been shown that other interactions distinct from the electron-nuclear contact interaction responsible for the Knight shift are relatively unimportant.

The major characteristics of the results are a very rapid broadening of the absorption with increased impurity content, coupled with a shift of the absorption. The shift is roughly proportional to the excess valence of the solute and is in every case decreased from its value in the pure metal; it is proportional to solute concentration within experimental error. These characteristics are consistent with the presence of the long-

* Present address: Department of Metallurgy, University of Illinois, Urbana, Illinois.
[1] T. J. Rowland, Phys. Rev. **119**, 900 (1960).
[2] J. Friedel, Phil. Mag. **43**, 153 (1952).
[3] A. Blandin, E. Daniel, and J. Friedel, Phil. Mag. **4**, 180 (1959).
[4] A. Blandin and E. Daniel, J. Phys. Chem. Solids **10**, 126 (1959).

range oscillations in conduction electron density previously noted by Friedel *et al.* Prior to the time the experimental results on the Knight shift in solid solutions of silver became available, the long-range oscillations were not considered in describing the charge distribution around solute atoms. The screening charge, i.e., the conduction electron charge accumulated in the immediate vicinity of the solute was usually calculated by the Thomas-Fermi method. This solution does not account properly for the long range effects associated with the scattering of the higher energy electrons ($k \neq 0$) in the Fermi sea. The relevant expressions derived from scattering theory will be presented in Sec. IV, together with the computed line shifts and second moments obtained from their use. These results will be compared with the corresponding experimental quantities in Secs. V and VI. Sections II and III contain discussions of the experimental methods and results, respectively, and conclusions are presented in Sec. VII.

II. EXPERIMENTAL METHOD

A Bloch (crossed coil) spectrometer was used for all of the measurements on silver and its alloys. The rf level at the sample was limited to 0.04 gauss or less in every case because of the onset of saturation. An audio modulation frequency ν_a of 20 cps was used in order to minimize distortion and phasing difficulties which arise when ν_a becomes comparable to either the line width or the inverse spin lattice relaxation time T_1^{-1}. The latter can be estimated from the Korringa relation[5] to be about 66 sec^{-1} for silver. To obtain useful absorption curves for the alloys, especially for the higher solute concentrations, a 90-sec output time constant followed the phase sensitive detector. The external field was swept through the resonance condition in every case and the spectrometer frequency ν_m was held constant by crystal control. A crystal stabilized Pound unit was used simultaneously to determine a reference field of 10 040.7 gauss corresponding to the resonance of pure silver metal at ν_m. All alloy resonance positions (fields) were measured with respect to this reference in order to eliminate effects of long term field drift. The reference field was determined by the absorption of deuterium in a small quantity of D_2O located about $\frac{3}{4}$ in. from the silver in the direction of the external field.

The alloys were prepared in about 50 g quantities by melting the weighed constituents together under argon in sealed quartz capsules, holding them 50–100°C above the melting point and periodically agitating them for about 2 hr, then air cooling them rapidly to a temperature just below the solidus. Subsequently they were annealed in order to smooth the small scale inhomogeneities in composition which arise during solidification. The silver was 99.999% Ag and the various solutes were also of high purity (Ga, In, Zn>99.999; Cu, As, Au, Cd, Ge, Sn>99.99; Tl>99.9; Sb>99.8).

The measurements were done on 200-mesh filings. Microscopic analysis of particle size distribution showed an average thickness of about 30 μ with about 80% of the filings under 50 μ. The worst situation with regard to skin depth occurs for pure silver, but here comparison with colloidal metal showed less than 0.05 gauss shift in the position of the derivative zero. To avoid errors in estimating the effect of skin depth a series of experiments on filings of copper was made from which a plot of t/δ vs Δ_e could be derived. Here t is particle thickness, δ is skin depth and Δ_e is the error in line position expressed as a fraction of the line width. The results clearly demonstrate that no systematic error can arise from this source in the present investigation. For the metals used the resistivity varies from about 1.6 μohm cm for pure Ag to 45 μohm cm for Ag-6 at.% Sb, and the corresponding t/δ (for 50 μ material at 2 Mc/sec) run from 1.1 to 0.2. Thus, as the solute concentration increases the possible source of error rapidly diminishes. Most of the filings were coated with AgS by immersion in an aqueous solution of K_2S although this was found to be unnecessary for the more concentrated alloys.

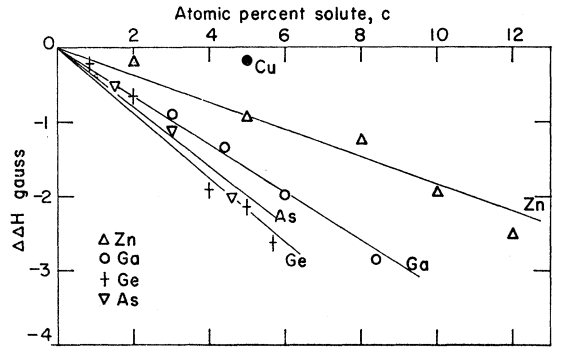

FIG. 1. The decrease in absolute Knight shift in gauss vs solute concentration for the fourth period elements Cu, Zn, Ga, Ge, and As. The absolute Knight shift ΔH_0 was 52.7 gauss and the external field 10 040.7 gauss. The slopes of the lines divided by ΔH_0 are compared with theory in Sec. V.

[5] J. Korringa, Physica **16**, 601 (1950).

III. EXPERIMENTAL RESULTS

Figures 1 and 2 show the change in the Knight shift vs composition for Ag^{109} with Zn, Ga, Ge, and As (Fig. 1) and Cd, In, Sn, Sb, and Tl (Fig. 2), respectively as solute. The data plotted are absorption derivative zeros. They are the result of from 5 to 12 independent measurements and, as can be seen in the figures, usually about 5 alloy compositions were used to determine the $\Delta\Delta H$ vs c dependence for any one solute. The standard deviation for single measurements and for the mean value of the shift were calculated for each alloy and were generally less than 10% of the shift. The error bars are omitted from the figures in the interest of clarity.

Two things are apparent from the data, namely, the change in the Knight shift $\Delta\Delta H$ of these alloys is never positive, i.e., the addition of solute always decreases the shift, and furthermore the decrease is at least closely

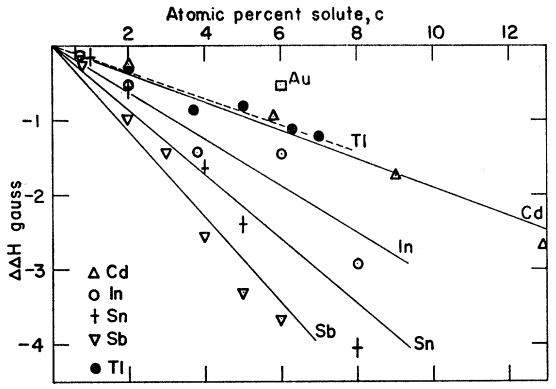

FIG. 2. The decrease in the absolute Knight shift ΔH_0 (52.7 gauss) for the fifth period elements Cd, In, Sn, Sb, and for Au and Tl. Comparison with Fig. 1 shows that with the exception of As and Sb the fourth and fifth period solute lines have the same slope, indicating the "charge only" character of the interaction giving rise to the shift.

proportional to the solute concentration. The slopes are also closely proportional to the solute valence and bear no obvious relationship to solute size, so the latter can apparently be neglected in the further analysis of the data.

A regularity in the data shows plainly in Figs. 1 and 2. At the lower solute concentrations the peak of the absorption curve (derivative zero) consistently falls below the line which best fits the plotted data. They would fall even farther below lines connecting the origin with the best high composition data. In two cases (0.8 at.% Ge and 1 at.% Sn), the *mean shift* was computed from the recorded derivative. In both cases the mean was found to lie on the line passing through the high concentration data. This is due to the marked asymmetry of the absorption of some of the dilute solutions. It was convenient to plot derivative zeros in Figs. 1 and 2, but it should be kept in mind that only for the high concentration data are these zeroes a good approximation to the mean value. At low concentrations the mean value always lies at a higher field than the derivative zero and thus corresponds to a greater decrease in the Knight shift. Within the experimental error the mean value thus goes linearly with composition, in agreement with theory. If it is assumed the best fit line passes through the two or three highest concentration points rather than all the points plotted then in the case of Ge, In, Sn, and Sb the experimental $-\Delta K/K_0 c$ are 0.86, 0.70, 0.95, and 1.20, respectively, (cf. Table I). These are the only solutes for which such a recalculation made a significant difference.

Plots of linewidth vs solute concentration appear in Figs. 3 and 4. It will be shown that these widths are the result of the inhomogeneous Knight shift. Nuclei at various distances from surrounding solute atoms are subjected to markedly different electron densities. The scatter results in a profusion of shifts interpreted as the width. The shape of the broadened silver absorption at

TABLE I. Experimental values of $-\langle\Delta K\rangle_{av}/K_0 c = -\Delta\langle\Delta H\rangle_{av}/\Delta H_0 c$ for comparison with calculated values using phase shifts from several sources.

	Experimental	Blatt	Square well	R' and Z' $\eta_2=0.11\eta_1$	R' and Z $\eta_2=0.11\eta_1$	R' and Z (9), $\eta_2=0$
Cu	0.07	0.009		0.20	0.12	
Au	0.21	(0.036)[a]		0.24	0.17	
Zn	0.35	0.142	0.151	0.63	0.58	
Cd	0.36	0.155	0.151	0.52	0.58	0.77
Ga	0.62	1.017	0.975	0.414	0.35_1	
In	0.60	0.835	0.975		0.35_6	0.41
Tl	0.34	0.798	0.975	0.444	0.34_9	
Ge	0.82	1.558	1.667	1.28	1.31	2.35
Sn	0.82	1.500	1.667	1.47	1.76	2.20
As	0.76	1.280	1.252	2.73	2.82	
Sb	1.09	1.370	1.252	2.52	2.70	3.08

[a] Huang's phase shifts were used, Proc. Phys. Soc. (London) **60**, 161 (1948).

the higher solute concentrations compares rather well with a gaussian curve. At lower concentrations (<3 at.%) there is often perceptible asymmetry and below 1 at.% solute there is marked asymmetry as discussed briefly above. This effect is most pronounced for the solutes of highest valence because their spectra are the most extended, that is, $\Delta\rho(r_i)/\rho_0$ is in general greater the higher the solute valence. Here $\Delta\rho(r_i)$ is the change in electron density at the ith neighbor a radial distance r_i from the solute, and ρ_0 is the initial unperturbed electron density.

The use of peak-to-peak line width δH_{pp} in Figs. 3 and 4 was dictated by the desire to plot actual experimental data rather than derived information and to approximate plots of experimental root second moment for comparison with theory. The symbol δH_{pp} represents the only use of the lower case delta for full line width in this paper. In every other case δH will refer to a half-width in order to facilitate comparison with the root

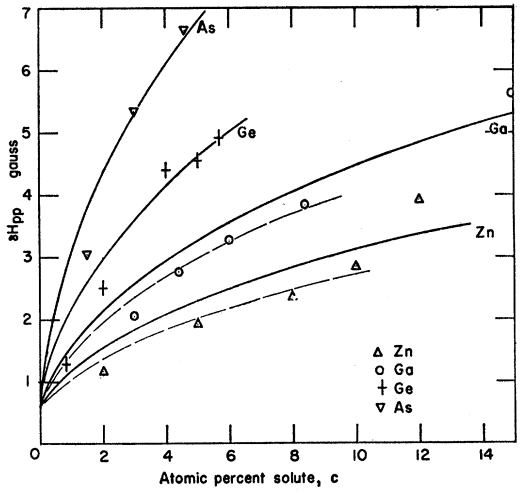

FIG. 3. Peak-to-peak line width of the fourth period elements as a function of solute concentration. The points above about 2% solute are fair approximations to twice the root second moment of the line. More dilute alloys are discussed in the text. The solid lines are parbolas best connecting all the data for a given element. The thin broken line is drawn through all Ga and Zn points except those of highest solute concentration.

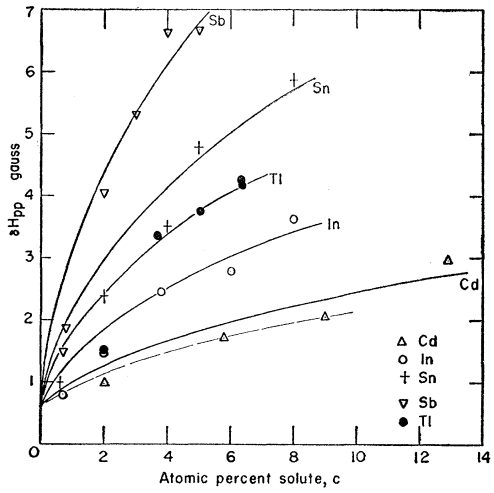

FIG. 4. Peak-to-peak linewidth of the fifth period elements and Tl. Super-position of Fig. 4 and Fig. 3 or perusal of Table II shows the overlap of Sb and As and Sn with Ge. The lower composition points would fall nearer the parabolas if in each case twice the true root mean square were plotted.

second moments. Again it is clear that the low solute concentration points (especially for high valence solutes) invariably lie below the best fit parabolae. The curves as drawn represent a good approximation to $2(\langle\delta H_e^2\rangle_{\rm av})^{\frac{1}{2}}$ at the high concentration where the absorption is gaussian; $(\langle\delta H_e^2\rangle_{\rm av})^{\frac{1}{2}}$ is the root second moment derived from the experimental data. At low solute concentrations δH_{pp} is not a good approximation to $2(\langle\delta H_e^2\rangle_{\rm av})^{\frac{1}{2}}$ and a plot of the latter should be made in order to present the most significant results for comparison with theory. In two cases (0.8 at.% Ge and 1 at.% Sn) the root second moments were computed in detail from the experimental curves. Twice this result brought the plotted point into significantly better agreement with the parabolae and it is reasonable to expect that all of the low concentration data would fall much nearer the curves of $\delta H_{pp}=2(\langle\delta H_e^2\rangle_{\rm av})^{\frac{1}{2}}$ if their second moments were to be computed. Fortunately, the least squares method, which was used to derive the parabolas plotted in Figs. 3 and 4, weights the high c points and makes the parabolas rather better approximations to the desired $2(\langle\delta H_e^2\rangle_{\rm av})^{\frac{1}{2}}$.

Several interesting observations can be made concerning Figs. 3 and 4. Comparing the two we find that the curves for Sb and As overlap and those for Sn and Ge overlap, i.e., their second moments are equal at equal compositions. After considering other sources of broadening in Sec. IV this fact will allow the conclusion to be made that the long-range oscillations in the electron density must be the entire cause of the width in these cases. The fine broken lines have been drawn through all of the points except the highest in solute concentration for Cd, Zn, and Ga. Again it is a least squares fit, but the point which seems most likely to be in error (because of the difficulty of measuring the width

TABLE II. Experimental and calculated values of the quantity $\Sigma_R[\Delta\rho(R)/\rho_0]^2$ contributed by the inhomogeneous Knight shift.

	Experimental	Blatt	Square well	R' and Z' $\eta_2=0.11\eta_1$	R' and Z $\eta_2=0.11\eta_1$	R' and Z (9) $\eta_2=0$
Cu	0.0016			0.0047	0.0019	
Au	0.006	(0.0004)[a]		0.0088	0.008	
Zn	0.009	0.003	0.003	0.028	0.024	
Cd	0.006	0.002	0.003	0.020	0.024	0.043
Ga	0.020	0.062	0.057	0.043	0.039	
In	0.014	0.042	0.057		0.032	0.045
Tl	0.026	0.040	0.057	0.031	0.038	
Ge	0.040	0.113	0.130	0.097	0.098	0.386
Sn	0.039	0.104	0.130	0.18	0.224	0.334
As	0.086	0.129	0.137	0.408	0.413	
Sb	0.087	0.105	0.137	0.38	0.388	0.502

[a] See footnote Table I.

of a very broad line) has been deleted. The recalculated experimental values of $\sum_R[\Delta\rho(R)/\rho_0]^2$ corresponding to the broken lines are 0.004, 0.007, and 0.016 for the Cd, Zn, and Ga, respectively, (cf. Table II).

The one solute which seems to broaden the absorption line much more than the other elements in its group is Tl; it may be that in this case that there is a second source of broadening which contributes significantly.

IV. ANALYSIS OF ABSORPTION LINE PARAMETERS IN SUBSTITUTIONAL SILVER ALLOYS

A. Knight Shift Contribution

The theory developed by Blandin, Daniel, and Friedel[3,4] will be used to analyze the Knight shift contribution to the results presented in Sec. III. In general, it can be said that any disturbance in the strict periodicity of the lattice will give rise to a redistribution of the conduction electron charge. Since the Knight shift is proportional to the electron density at the Fermi level at the nuclei, it is possible to determine, at least at these few isolated points, the change in Fermi charge density which has accompanied the disruption in periodicity. The insertion of a point imperfection on a lattice site is particularly easy to handle theoretically using well developed scattering theory and ignoring the lattice symmetry. The scatterer can be considered a spherical square well and the incident and scattered waves expanded in terms of spherical Bessel functions j_l and Neumann functions n_l to arrive at the change in the relative Knight shift $\Delta K_i=\Delta(\Delta H/H_0)_i$ at a site a distance r_i from the scatterer. Since the Knight shift is proportional to the Fermi electron density at a nucleus, the proportional change in the relative Knight shift caused by the scattered wave is just

$$(\Delta K/K_0)_i=(\Delta\rho/\rho_0)_i=\Delta\rho(r_i)/\rho_0,$$

where $K=\Delta H/H_0$ and ρ_0 is the unperturbed conduction electron density for electrons of Fermi momentum k. The expression for $\Delta\rho(r_i)/\rho_0$, the relative change in the electron density at a distance r_i from the scatterer is[4]

$$\Delta\rho(r_i)/\rho_0=\sum_l[\alpha_l(kr_i)\sin^2\eta_l+\beta_l(kr_i)2\sin\eta_l\cos\eta_l], \quad (1)$$

where

$$\alpha_l(kr_i)=(2l+1)[n_l^2(kr_i)-j_l^2(kr_i)],$$

and

$$\beta_l(kr_i)=-(2l+1)n_l(kr_i)j_l(kr_i),$$

the $n_l(kr_i)$ and $j_l(kr_i)$ being the appropriate spherical Neumann and Bessel functions, respectively, and η_l is the phase shift produced by the perturbing potential of the solute in the lth spherical component of an incident plane wave.

From the computed $(\Delta\rho/\rho_0)_i=(\Delta K/K_0)_i$ theoretical expressions for $\langle\Delta K\rangle_{\rm av}$ and $\langle\delta K^2\rangle_{\rm av}$, the mean change in Knight shift and the mean square deviation from the mean, can be derived. The shift *data* is presented in Figs. 1 and 2 as $\Delta\langle\Delta H\rangle_{\rm av}$ vs c, where $\Delta\langle\Delta H\rangle_{\rm av}=H_0\langle\Delta K\rangle_{\rm av}$. The measurements were of the change in field of the line center occurring when the silver was alloyed. To find $\langle\Delta K\rangle_{\rm av}$ we assume a *random* dilute solid solution and neglect multiple scattering processes. Sum the effect of all n solute nuclei on all N solvent nuclei; the mean change for the jth silver atom, due to all n is just

$$\Delta K_j=\sum_{i=1}^{n}\Delta K(r_{ij})=K_0\sum_{i=1}^{n}\Delta\rho(r_{ij})/\rho_0.$$

Here r_{ij} is the distance between solvent j and solute i. This must be averaged over all N silver atoms and is

$$\frac{\langle\Delta K\rangle_{\rm av}}{K_0}=\frac{1}{N}\sum_j^N\sum_i^n\frac{\Delta\rho(r_{ij})}{\rho_0}.$$

Because of the statistical equivalence of the solute atoms this can be written

$$\frac{\langle\Delta K\rangle_{\rm av}}{K_0}=\frac{n}{N}\sum_j^N\frac{\Delta\rho(r_j)}{\rho_0}=\frac{n}{n+N}\sum_R\frac{\Delta\rho(R)}{\rho_0}=c\sum_R\frac{\Delta\rho(R)}{\rho_0},\quad(2)$$

where r_j denotes the position of the jth solvent atom, $\sum_R$ is the sum over *all* lattice sites except the origin, and c is the solute concentration in atomic fraction. It is $\langle\Delta K\rangle_{\rm av}/K_0c=\Delta\langle\Delta H\rangle_{\rm av}/c\Delta H_0$ obtained experimentally which is to be compared with the same quantity $\Sigma_R\Delta\rho(R)/\rho_0$ obtained from theory. The lower case delta will be used to indicate shifts from the mean K while the capital delta will indicate shifts from K_0, the relative Knight shift of the pure solvent. It is most common to consider $\langle\Delta K\rangle_{\rm av}=\bar{K}-K_0$ and $\langle\delta K^2\rangle_{\rm av}=\langle K^2\rangle_{\rm av}-\bar{K}^2$. The latter gives the line width directly for Gaussian lines. It can be shown [using the arguments leading to ΔK in (2)] that $\langle\delta K^2\rangle_{\rm av}=c(1-c)K_0^2\sum_R[\Delta\rho(R)/\rho_0]^2$ and thus

$$\langle\delta H_k^2\rangle_{\rm av}=c(1-c)\Delta H_0^2\sum_R[\Delta\rho(R)/\rho_0]^2,\quad(3)$$

where ΔH_0 is the absolute Knight shift in gauss of the pure solvent. The sum again is over all lattice sites, each term being given by Eq. (1). This second moment is in gauss^2 and represents the contribution due only to the long-range oscillations of the electron density.

To compare the observed line widths with those predicted by (3) it is necessary to subtract from the observed values the contributions of the pure metal and any additional contributions introduced by dipolar and indirect exchange mechanisms. Although the data show only peak-to-peak line widths δH_{pp}, comparison of various higher concentration experimental lines were made with gaussian curves and the agreement was sufficiently close to allow use of the usual second moment approximations at least in the region of high solute concentration. We assume that the total experimental second moment $\langle\delta H_e^2\rangle_{\rm av}$ is composed of the Knight shift, indirect exchange, and dipolar contributions so that

$$\tfrac{1}{2}\delta H_{pp}\cong(\langle\delta H_e^2\rangle_{\rm av})^{\frac{1}{2}}=[\langle\delta H_K^2\rangle_{\rm av}+\langle\delta H_x^2\rangle_{\rm av}+\langle\delta H_d^2\rangle_{\rm av}]^{\frac{1}{2}}.\quad(4)$$

The exchange and dipolar contributions for every alloy have been evaluated as described in the following paragraphs.

B. Dipolar Contribution

The dipolar width of the species being observed (Ag^{109}) is composed of contributions from all $I\neq0$ isotopes present; for a binary alloy this includes all $I\neq0$ solvent nuclei and solute nuclei present in solution. The second moment under these circumstances is given by

$$\begin{aligned}\langle\delta H_d^2\rangle_{\rm av}=\{&\tfrac{1}{3}I(I+1)\gamma_{109}^2\hbar^2p_{109}(1-c)\\&+(4/15)I(I+1)\gamma_{109}^2\hbar^2p_{109}(1-c)\\&+(4/15)I_{107}(I_{107}+1)\gamma_{107}^2\hbar^2p_{107}(1-c)\\&+(4/15)I_i(I_i+1)\gamma_i^2\hbar^2p_ic\}\sum_j r_{0j}^{-6},\end{aligned}\quad(5)$$

where the notation is standard; I is the spin of Ag^{109}, γ_{109} the gyromagnetic ratio of Ag^{109}, $\hbar$ equals Planck's constant divided by 2π, and p is the isotopic abundance of the species denoted by its subscript. The other symbols are similarly defined for the isotope shown by the subscript, i being used for the solute isotope. The sum over r_{0j} is over all lattice sites of the silver lattice and has the value 2.484×10^{46} cm^{-6}. The first term in the bracket above is the quantum mechanical "mutual spin flip" term derived by Van Vleck, the rest are the static field contributions. When solute atoms are added the contribution of the first term is removed (there cease to be "like" neighbors). If the contribution of n silver atoms are removed from the term for every solute atom added the number of silvers contributing to it will drop as $(1-c)^n$ and the term will contain a $(1-c)^n$ factor. Since $I=I_{107}=\frac{1}{2}$, Eq. (5) can be written

$$\begin{aligned}\langle\delta H_d^2\rangle_{\rm av}=\{&\tfrac{1}{4}\gamma_{109}^2\hbar^2p_{109}(1-c)^{n+1}\\&+\tfrac{1}{5}\gamma_{109}^2\hbar^2p_{109}(1-c)+\tfrac{1}{5}\gamma_{107}^2\hbar^2p_{107}(1-c)\\&+(4/15)I_i(I_i+1)\gamma_i^2\hbar^2p_ic\}\sum_j r_{0j}^{-6}.\end{aligned}\quad(6)$$

This expression was used to compute $\langle \delta H_d^2 \rangle_{av}$ for several alloys; n was set equal to 12, 30, 40, and 50 for solutes of $Z=1$, 2, 3, and 4 respectively. It became clear that $\langle \delta H_d^2 \rangle_{av}$ was not the determining factor in the linewidth, and for the balance of the compositions a simpler form of (6) was used wherein we let $p_{107}=p_{109}=\frac{1}{2}$ and $\gamma_{107}=\gamma_{109}$. Then (6) could be written

$$\langle \delta H_d^2 \rangle_{av}=\{\tfrac{1}{5}\gamma_{109}^2\hbar^2(1-c)[1+\tfrac{5}{8}(1-c)^n] + (4/15)I_i(I_i+1)\gamma_i^2\hbar^2 p_i c\}\sum_j r_{0j}^{-6}. \quad (6a)$$

The latter form was used for the majority of $\langle \delta H_d^2 \rangle_{av}$ values.

C. Indirect Exchange

The indirect exchange contribution to the second moment is in every case much more important than the direct dipolar contribution, often exceeding it by a factor of 10 or more. According to Van Vleck,[6] the exchange broadening is composed of terms of the type

$$\langle \delta H_x^2 \rangle_{av}=\frac{1}{3\hbar^2\gamma_{109}^2} I'(I'+1)\sum_{j'} \tilde{A}_{ij'}^2, \quad (7)$$

where $\langle \delta H_x^2 \rangle_{av}$ is the exchange contribution to the second moment of the absorption and $\tilde{A}_{ij'}$ is the exchange constant between the solvent species i and the unlike primed species j'. Always assume we are looking at the resonance of Ag^{109} so that $i=109$ in *every* case and can be dropped as a subscript.

For a silver alloy with one solute isotope j' and the one "unlike" silver isotope Ag^{107} Eq. (7) leads to

$$\langle \delta H_x^2 \rangle_{av}=\frac{1}{3\hbar^2\gamma_{109}^2}\Big\{ I_{109}(I_{109}+1)(1-c) \times[1-(1-c)^n]p_{109}\sum_R [\tilde{A}_{109'}(R)]^2 + I_{107}(I_{107}+1)p_{107}(1-c)\sum_R [\tilde{A}_{107}(R)]^2 + I_{j'}(I_{j'}+1)cp_{j'}\sum_R [\tilde{A}_{j'}(R)]^2\Big\}, \quad (8)$$

where here the isotopic abundance p and concentration have been included and the sums $\sum [\tilde{A}_{j'}(R)]^2$ are over all lattice sites. $\tilde{A}_{107}(R)$ is the exchange constant between Ag^{107} and Ag^{109}, and $\tilde{A}_{j'}(R)$ is appropriate to Ag^{109} and the solute species j'. The first term takes into account the Ag^{109} nuclei which have no effect on the second moment when they are all identical but which contribute to it when the solute species are added and the individual Ag^{109} resonances become nonidentical resonances $Ag^{109'}$. Silver nuclei within n atoms of the solute are assumed to have their absorptions shifted by more than the line width of pure silver. The n values are those under (6). Letting $I_{109}=I_{107}=\frac{1}{2}$, $p_{107}=p_{109}=0.5$, and $\tilde{A}_{109'}(R)=\tilde{A}_{107}(R)$ for simplification, (8) becomes

$$\langle \delta H_x^2 \rangle_{av}=\frac{1}{4\hbar^2\gamma_{109}^2}(1-c)[1-0.5(1-c)^n]\sum_R [\tilde{A}_{107}(R)]^2 + \frac{1}{3\hbar^2\gamma_{109}^2} I_{j'}(I_{j'}+1)cp_{j'}\sum_R [\tilde{A}_{j'}(R)]^2. \quad (9)$$

Each $\tilde{A}_i(R)$ can be written in terms of its constant part and its radially dependent part, that is

$$\tilde{A}_{j'}(R)=A_{j'}F(R)=A_{j'}(2kR\cos 2kR-\sin 2kR)/R^4), \quad (10)$$

where

$$A_{j'}=\Omega^2 m^*\xi_{109}\nu_a(109)\xi_{j'}\nu_a(j')/2\pi(2I_{109}+1)(2I_{j'}+1).$$

The volume of the unit cell of silver is Ω, the effective electron mass is m^*; $\xi=P_F/P_a$ is the ratio of the electron density at the nucleus averaged, in effect, over the Fermi surface[7] in the metal to the density at the nucleus in the free atom. With few exceptions the hyperfine coupling constant $a(s)$ for the s electron in the atom, where $\nu_a(j')=a_{j'}(s)(I_{j'}+1)$, is not known to high accuracy. Thus the factors m^*, $\xi_{j'}$, and $\nu_a(j')$ are all subject to some uncertainty and the accurate evaluation $A_{j'}$ is not in fact possible. The atomic ground-state hyperfine splittings $\nu_a(j')$ can be estimated, ξ is a numerical factor of order 1, and we will let $m^*=m$ to proceed with the evaluation in Sec. VI.

V. COMPARISON OF THEORY AND EXPERIMENT—SHIFT

The theoretical expression (2) for the shift was evaluated out to the 15th neighbor position and from $l=0$ to either 2 or 3 using phase shifts derived in a variety of ways. The spectrum of $(\Delta K/K_0)_i$ was computed in each case, and then $\langle \Delta K \rangle_{av}/K_0 c=\sum_i n_i(\Delta K/K_0)_i$, was evaluated; here n_i is the number of atoms in the shell i. The results are listed in Table I, in which the columns have the following significance: the second column was computed using Blatt's[8] phase shifts; the third used phase shifts for a square well potential *not* corrected for size. For both of these, η_l for $l=0$ to 3 were used. The column headed R' and Z' used semi-empirical phase shifts derived from simultaneous solution of resistivity and Friedel sum rule equations *with* size correction applied to sum rule and $\eta_2=0.11\eta_1$ in every case; the R' and Z column is the same *without* size correction. The column referring to (9) used the semi-empirical phase shifts quoted by Giffels, Hinman, and Vosko.[9] These workers allowed $\eta_2=0$ in every case.

The use of the sum rule and resistivity to derive "semi-empirical" phase shifts[10] is a straightforward

[6] J. H. Van Vleck, Phys. Rev. **74**, 1168 (1948).

[7] M. A. Ruderman and C. Kittel, Phys. Rev. **96**, 99 (1954).

[8] F. J. Blatt, Phys. Rev. **108**, 285 (1957).

[9] C. A. Giffels, G. W. Hinman, and S. H. Vosko, Phys. Rev. **121**, 1063 (1961).

[10] W. Kohn and S. H. Vosko, Phys. Rev. **119**, 912 (1960).

procedure to which which two minor variations were applied to arive at the present set of phase shifts η_l necessary to compute the Knight shift by (1). The residual resistivity of a dilute monovalent alloy is given by

$$R'=\frac{2hc}{e^2k}\sum_{l=1} l\sin^2(\eta_{l-1}-\eta_l), \tag{11}$$

where c is the atomic fraction solute. The Friedel sum rule,[11,2] which guarantees the compensation of the excess charge on the ion by a shielding charge of conduction electrons, places the requirement

$$Z'=(2/\pi)\sum_l (2l+1)\eta_l, \tag{12}$$

on the phase shifts. Here Z' is the *size-adjusted* valence difference according to Blatt,[8] Table III, column N. The symbol Z will be used when no adjustment for size has been made, i.e., $Z=1$, 2, 3, 4, and 5. Clearly from two independent relations for η we should get two phase shifts, however, a perusal of Blatt's phase shifts shows that $\eta_2=(0.11\pm0.03)\eta_1$, hence in the above equations η_2 was set equal to $0.11\eta_1$ and three phase shifts obtained. It should be emphasized that the phase shift η_2 is included because of its strong influence on the s shift η_0 through the Friedel sum rule. It is not particularly important to have η_2 for the purpose of our calculations.

The experimental values of line shift in the first column of Table I are derived from Figs. 1 and 2; they are the slopes of the best straight lines drawn through the data points as discussed in Sec. III. Agreement between calculated and measured $\langle\Delta K\rangle_{\rm av}/K_0c$ is in no sense striking. In some cases there are trends which appear significant, such as the definite increase of both the calculated and measured values with valence. The two values generally differ by a factor of about 2, and not always in the same direction. It was not possible to satisfy the equations for the phase shifts, using the residual resistivity and Friedel sum rule, for Zn and Cd. This probably explains their relatively high values in Table I. The phase shifts of Blatt appear to offer somewhat better agreement with experiment that those derived in other ways, however, it seems probable that the semi-empirical phase shifts should actually be the most realistic, and that therefore it may be better when comparing theory with experiment to use the line shifts derived from the latter either with or without size correction. Comparison of the Blatt and square well columns or the R' and Z' and R' and Z columns in Table I will show that for the present purposes the effect of size is not great. It is by use of the R' and Z column that the factor of roughly 2 was arrived at above.

Examples of the sort of spectra obtained are displayed in reference 4. The individual components $(\Delta\rho/\rho_0)_i$ undergo shifts roughly proportional to the solute valence, thus it is not surprising to find the mean shifts of the composite structure shifting almost linearly with solute valence.

[11] J. Friedel, Suppl. Nuovo cimento 7, 287 (1958).

Perhaps it should be pointed out that the Knight shift is the only mechanism which we need to consider in searching for the source of line shift, or asymmetry in the absorption of Ag^{109}. All other mechanisms would cause symmetric broadening about the spectral lines of the resonance, but the *mean* value must be determined by the electron density at the nuclei. Whereas a considerable amount of effort is spent in Sec. VI showing that the width is due to the Knight shift rather than some other mechanism, we need only consider this one source of shift.

VI. COMPARISON OF THEORY AND EXPERIMENT—WIDTH

It has been suggested above that with the possible exception of the effect of Tl the inhomogeneity in the Knight shift is the major source of width in the silver alloys examined. Figures 3 and 4 show the peak-to-peak measured widths in these alloys. The contribution of the dipolar and/or exchange mechanisms to the linewidths of Ge, Sn, and As are unquestionably negligible. If their widths are assumed to be characteristic of the contribution of the inhomogeneous Knight shift alone, then it is clear that the group 3 elements and Sb (for which the indirect exchange mechanism might conceivably contribute) are in fact not substantially indirect exchange broadened either. To quantitatively analyze the total width of the various absorptions the required $A_{j'}(R)$ and then $\langle\delta H_d{}^2\rangle_{\rm av}+\langle\delta H_x{}^2\rangle_{\rm av}$ were computed[12] for every alloy on which measurements were made. Only for those containing Ga, In, Tl, and Sb is the exchange term large enough to affect the observed width. It may be then that the rather large scatter in the shift data for these elements is caused by some indirect exchange contribution to their width. As was pointed out above, it is possible to rationalize these widths; however, there is no way to determine a unique choice for the quantities entering into the product $m^*\xi_{j'}\nu_a(j')$. Using the $a(s)$ from Knight's[12] Table III the quantity $\langle\delta H_d{}^2\rangle_{\rm av}+\langle\delta H_x{}^2\rangle_{\rm av}$ evaluated for 6 at.% Ga, In, Tl, and Sb is 1.5, 10.9, 6.7, and 8.1 gauss^2, respectively. This is considerably too high and not even in the correct order to explain the experimental data; the value of $A_{j'}$ must be in error. The fact that the group III elements lie together (see Table II) is some indication that the dominant source of broadening is the Knight shift inhomogeneity. There are further indications of the dominant role of the Knight shift as the source of width; arsenic introduces only a very small exchange broadening, yet its width is exactly the same as that of Sb showing that any exchange contribution of the Sb must certainly not contribute significantly. It is unreasonable to assume that the agreement between As and Sb is the result of a fortuitous combination of Knight broadening

[12] Hyperfine constants were taken from W. D. Knight, Solid-State Physics, edited by F. Seitz and D. Turnbull (Academic Press, Inc., New York, 1956), Vol. 2, p. 93 or H. Kopfermann, *Nuclear Moments* (Academic Press Inc., New York, 1958).

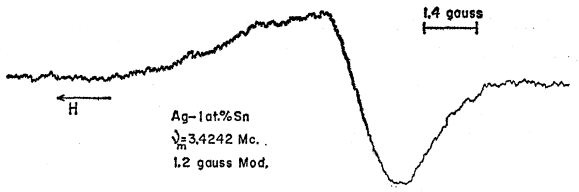

FIG. 5. Absorption curve of an alloy of silver containing 1 at. % Sn. External field strength about 17 200 gauss. The extra bump has always been found on the high-field (low Knight shift) side where the first strong line in the computed spectrum generally falls. This sample is so concentrated that considerable broadening of the low-field side has already occurred. No side lines have been seen in dilute alloys of Sb.

and exchange broadening. The rather precise agreement of Ge with Sn, neither of which cause important exchange, argues in favor of this interpretation of the As and Sb data.

The experimentally observed *peak-to-peak* line widths in Figs. 3 and 4 are plotted together with the parabolae which best pass through the data according to a least squares analysis. The primary reason for calculating the curves was to obtain the best experimental value of $\sum_R[\Delta\rho(R)/\rho_0]^2$ to compare with the computed theoretical values. The curves have the equations $(\frac{1}{2}\delta H_{pp})^2=\langle\delta H_{\mathrm{Ag}}^2\rangle_{\mathrm{av}}+\langle\delta H_k^2\rangle_{\mathrm{av}}$ where $\langle\delta H_k^2\rangle_{\mathrm{av}}$ can be expressed as $c(1-c)\Delta H_0^2\sum_R[\Delta\rho(R)/\rho_0]^2$. Here δH_{pp} is the peak-to-peak width of the derivative curves $\langle\delta H_{\mathrm{Ag}}^2\rangle_{\mathrm{av}}$ is the square of the half-width of pure Ag and ΔH_0 is the absolute Knight shift. The terms $\langle\delta H_d^2\rangle_{\mathrm{av}}$ and $\langle\delta H_x^2\rangle_{\mathrm{av}}$ which contained $\langle\delta H_{\mathrm{Ag}}^2\rangle_{\mathrm{av}}$ have now been dropped. The least squares analysis provides the best experimental value for $\Delta H_0^2\sum_R[\Delta\rho(R)/\rho_0]^2=A$. Hence the experimental result for the sum is just $A/\Delta H_0^2$. This value is given in the first column of Table II with the other entries being the computed $\sum_R[\Delta\rho(R)/\rho_0]^2$ using the various phase shifts described in connection with Table I. To obtain a rough quantitative notion of the extent of the agreement between theory and experiment the fifth column (R' and Z) was divided by the first for each element. These quotients range from about 1.5 to 6, their square roots from 1.2 to 2.4. The theoretical root second moment is thus too large by a factor of roughly 2, as the shift was, and thus it seems highly probable that there is no source of width or shift which cannot be explained by the long-range oscillations in this composition range. The fact that the work of Drain[13] indicates no curvature of ΔH vs Cd concentration over a much larger composition range than was investigated in the present study also indicates that no additional source of shift becomes operative at higher solute concentrations. If there were another cause of shift we would expect, during its onset, and assuming it is linear with composition, a break connecting two straight lines within the Cd solid solubility range. The additional shift in mind might be caused by linear changes in one of the factors entering into the Knight shift, i.e., either χ_p or $\langle|\psi_F(0)|^2\rangle$ purely because of the change in electron concentration of the more concentraded solutions, or the additional shift might indicate a marked change in the band structure. If there were another source of mean line shift then one would expect the conflict with theory to be greater in the case of shift than for the width. Since they differ from the calculated values (which can only be considered valid within a factor of two) by approximately the same factor in each case, it can be assumed that no other significant cause of shift is present.

The most dilute alloys demand special attention. Since their Ag^{109} absorptions are asymmetric it should be possible to obtain more information about the outlying spectral lines $(\Delta K/K_0)_i$ by careful analysis of the line shape. In many of the recordings of the absorption derivative a definite bump or plateau was visible on the high field side of the resonance. An example is shown in Fig. 5. Furthermore, some work was done on alloys of less than one per cent solute concentration in a magnetic field of 17 200 gauss. This improved the resolution of the side peaks somewhat because the central part of the line is still largely contributed by pure silver, the width of which is not field dependent. A discussion of the manner in which the data from the most dilute alloys was handled appears in Sec. III. No attempt was made at this time to identify the high field spectral line causing the bulk of the asymmetry, but it is probably that of the nearest neighbor since its spacing from the pure silver resonance is nearly always greater than any other.

VII. DISCUSSION AND CONCLUSIONS

The present explanation of the change in the Knight shift brought about by alloying a pure metal ignores the quantities which were so hopefully pursued in earlier studies. The original experiments on alloys, and most of those done since, were performed with the idea of deriving from the results the density of states at the Fermi surface $n(E_F)$. This is of course *not* a function of position in the bulk metal.

The electron density per unit energy and volume of electrons near the Fermi level can be written

$$\rho(E_F,r)=n(E_F)\psi_k^*(r)\psi_k(r), \tag{13}$$

$n(E_F)$ being the number of electronic states per unit energy and volume near the Fermi surface, and $\psi_k(r)$ being the wave function of a conduction electron near the Fermi surface. The Knight shift is directly proportional to $\rho(E_F,r)$, being just

$$\Delta H=(8\pi/3)\beta^2\rho(E_F,r_i)H_0, \tag{14}$$

where r_i now denotes the positions of the nuclei and β is the Bohr magneton. In a pure metal all nuclei are equivalent and the expression for ρ becomes $\rho(E_F,r_i)=n(E_F)\langle|\psi_k(0)|^2\rangle$, the wave functions at the various nuclei are identical and the interpretation of (14) is clear. In the pure solvent metal it is at least sometimes

[13] L. E. Drain, Phil. Mag. 4, 484 (1959).

possible to calculate $P_F=\langle|\psi(0)|^2\rangle_F$ or P_F/P_A where P_A is the probability density at the nucleus of an s electron in the like free atom. An experimental value for P_A can sometimes be obtained from the hyperfine splitting. If P_F is computed, a value for $n(E_F)$ is of course forthcoming. The presence of solute atoms complicates the meaning of (13) somewhat and in turn makes the Knight shift very much more difficult to interpret. Possibly the main feature to stress is the constancy of $n(E_F)$ throughout the alloy; we see then that the localized effects are in $P_F(R)$, the probability density at the nucleus at R, and that whatever simultaneous changes there may be in $n(E_F)$ are masked by the dominant role of the first few oscillations. Writing the Knight shift in the form

$$\Delta H/H=(8\pi/3)\beta^2 n(E_F)P_F(R), \qquad (15)$$

it is clear that without some assumptions or auxiliary information, it is not possible to obtain knowledge concerning either $n(E_F)$ or $P_F(R)$ alone. The present study makes no attempt to derive either of the quantities, but is occupied with the change in their product only. An important observation concerning this product is the localization of the perturbation which it describes. The localized influence of the solutes was considered by Drain[13] in explaining the linewidths he observed in Ag-Cd alloys; it was not considered by Henry.[14]

Dilute solutions show the effect of screening most clearly. In this case there are some silver nuclei which are free of the effects of solutes, while others are in the vicinity of the solute atom and may be strongly affected. The Thomas-Fermi model would, of course, predict far less effect on the silver resonance and the shift would be in the opposite direction from that actually observed. This fact is sufficient proof of the presence of the long-range oscillations; also it is obvious that any smooth change in electron-to-atom ratio could not bring about the line shape observed for the dilute alloys, an example of which is shown in Fig. 5. This argument can in fact be extended to all of the broad lines observed for the solute concentrations studied. Clearly if the electrons were leaving the solute and merely increasing the bulk electron-to-atom ratio the line width would not increase; there would instead be a continuous shift of the resonance characteristic of pure silver except for *small* dipolar and exchange effects which we have evaluated. As the solutions grow more concentrated, and the electron distributions which surround the solutes overlap, the electron-to-atom ratio regains meaning in the traditional sense. In that sense it is surely correct to postulate a change in the shape of the band as the solute concentration is increased. The lengthy discussion of the noble metal Fermi surfaces and electronic properties by Cohen and Heine[15] points out that although the Knight shift is proportional to $n(E_F)$ a peak in the $n(E)$ curve may not be observed because the wave function on the zone faces which is responsible for the break in the $n(E)$ curve are p-like states and do not contribute to the Knight shift. Essentially then the Knight shift would be expected to vary smoothly even through a break in the $n(E)$ curve. This argument hinges on the shape of the Fermi surface in silver which is now thought to be nearly spherical[15] and probably touching the Fermi surface.[16]

Other considerations are the effects of core polarization[17] and the anisotropic Knight shift. The former should not affect our results here because we consider only the relative changes in the Knight shift. The core polarization would be expected to contribute to the absolute value of the Knight shift in the pure metal. The change in core polarization upon introduction of a solute atom should be proportional to the original core polarization to first order. The possibility of having a significant contribution from the anisotropic Knight shift has been considered.[18] It was found that the contribution to the width from this source would amount to less than ten per cent of the *change* in the Knight shift ΔK. The physical mechanism for this process would be a polarization of the silver cells neighboring a solute causing the same effect as has been previously noted in the pure anisotropic metals Sn and Cd.

ACKNOWLEDGMENTS

During the composition of this paper Dr. B. A. Green and Professor S. H. Vosko contributed their assistance and encouragement, for which I am sincerely grateful. It is a pleasure also to acknowledge the help of Mr. J. R. Radecki in conducting the experiments. We are indebted to the U. S. Atomic Energy Commission for partial support of this work.

[14] W. G. Henry, Proc. Phys. Soc. (London) **76**, 989 (1960).

[15] M. H. Cohen and V. Heine, Suppl. Phil. Mag. **7**, 395 (1958).

[16] R. W. Morse in *The Fermi Surface* (John Wiley & Sons, Inc., New York, 1960), p. 214.

[17] M. H. Cohen, D. A. Goodings, and V. Heine, Proc. Phys. Soc. (London) **73**, 811 (1959).

[18] S. H. Vosko (unpublished calculation).